

Steric and electronic effects on mesophase stability of segmented liquid crystalline polymers with arylazomethine pendant groups

Sandra A. Hernández¹, Yong-Hong Yang², Qi-Feng Zhou², Raúl O. Garay¹(✉)

¹ INIQA, Universidad Nacional del Sur, Avenida Alem 1253, 8000 Bahía Blanca, Argentina

² Department of Chemistry, Peking University, Beijing 100871, People's Republic of China
e-mail: rgaray@criba.edu.ar, Fax: 54-291-459 5187

Received: 10 April 2000/Revised version: 27 June 2000/Accepted: 5 July 2000

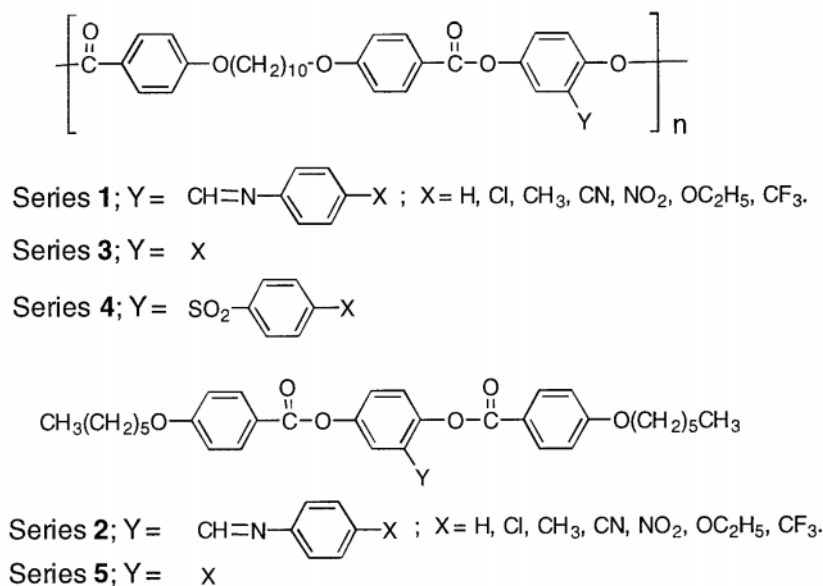
Summary

The synthesis and thermotropic behavior are reported for a series of polyesters, **1**, and its model compounds, **2**, which bear a N-arylazomethine pendant group with *para*-substituents in order to evaluate electronic and steric effects on mesophase stability of segmented LCP with Y-shaped mesogens. Substituent effects on these polymer series and model compound series are dominated by steric effects. The results suggest that due to the conformational flexibility of the azomethine group this type of macromolecules cannot be strictly considered as Y-shaped segmented liquid crystal polymers. It was also concluded that when steric effects are predominant the mesomorphic behavior of model compounds can be used to estimate polymer nematic mesomorphic properties.

Introduction

Most of liquid crystalline compounds, both low-molecular-weight and polymeric, have the conventional rod-like structure [1]. However, mesomorphic behavior it is not restricted to calamitic mesogens [2]. Thus, symmetric molecular broadening eventually leads to discotic and X-shaped mesogens while asymmetric broadening of mesogens produces T- or Y-shaped mesogens. Incorporation of these two-dimensional mesogenic units in a polyester main chain produces LCP materials with unusual architecture [3-5]. The rheology and properties of these polymers should be much different than those of conventional main chain liquid crystal polymers. Moreover, the poor lateral strength of liquid crystal polymer fibers may be improved using these unconventional structures [6].

However, the bulky side groups will diminish interchain interactions by virtue of its bulkiness though their polarity may also enhance electronic interchain interactions. Since the thermotropic behavior of segmented LCPs with Y-shaped mesogens is not well established, we synthesized a series of polyesters **1** and their model compounds **2**, bearing an N-arylazomethine pendant group with a *para*-substituent in order to evaluate the electronic and steric effects on mesophase stability (Scheme 1). In addition, their thermotropic behavior was compared with literature data that describes the mesomorphic properties of segmented liquid crystal polyesters **3** [7,8,9,10] and series **4** [11] and the model compound series **5** [12].



Scheme 1

Experimental

All melting points are uncorrected. Elemental analysis were made in the University of Massachusetts Microanalytical Laboratory. ¹H NMR and ¹³C NMR spectra were recorded on a Varian XL200 spectrometer. The *para*-substituted anilines, 2,5-dihydroxybenzaldehyde and *para*-*n*-hexyloxybenzoyl chloride were obtained commercially (Aldrich). 1,10-Bis(4'-chloroformylphenoxy)decane, **6**, was prepared according to a method previously described [13].

General procedure for the synthesis of N-(2,5-dihydroxybenzylidene)-para-substituted-anilines, 7a-g, given for 7a [X = H]. A mixture of 2,5-dihydroxybenzaldehyde (2.5 g, 18.1 mmoles) was dissolved in dry methanol (5ml) under argon and then a solution of the *p*-substituted aniline (18.1 mmoles) in dry methanol (10 ml) was added at room temperature. After one hour the temperature was increased to 60 °C for half an hour. A dark red precipitate was isolated by filtration after the reaction mixture was cooled to 10 °C. The solid was recrystallized from a mixture of benzene:tetrachloroethane (5:2) and washed with pentane. Yield: 65 %; m.p.: 142-144 °C. ¹H NMR (Acetone-d₆): 12.46 (s, 1H, OH), 8.79 (s, 1H, HC=N), 7.97 (s, 1H, OH), 7.5-7.3 (m, 5H, aromatic H), 7.05 (d, J = 2.5 Hz, 1H, aromatic H), 6.96 (dd, J = 8.8 Hz and J = 2.5 Hz, 1H, aromatic H), 6.83 (d, J = 8.8 Hz, 1H, aromatic H). ¹³C NMR (Acetone-d₆): 164.6, 155.6, 150.7, 149.8, 130.4, 127.8, 122.3, 122.2, 120.3, 118.6, 118.4. Anal. calcd. for C₁₅H₁₁NO₂: C 73.23, H 5.20, N 6.57. Found: C 73.56, H 5.30, N 6.55.

7b [X = Cl]. *N*-(2,5-dihydroxybenzylidene)-*p*-chloroaniline. An orange solid was isolated from the reaction mixture by filtration, washed with pentane and recrystallized twice from absolute ethanol in an ice-water bath. Yield: 82 %; m.p.: 164 °C. ¹H NMR (Acetone-d₆): 12.25 (s, 1H, OH), 8.79 (s, 1H, HC=N), 8.00 (s, 1H, OH), 7.45 (m, 4H, aromatic H), 7.04 (d, J = 2.9 Hz, 1H, aromatic H), 6.98 (dd, J = 8.7 Hz and J = 2.9 Hz, 1H, aromatic H), 6.82 (d, J = 8.7 Hz, 1H, aromatic H). ¹³C NMR (Acetone-d₆): 165.3, 155.8, 150.9, 148.8, 133.0, 130.6, 124.2, 122.7, 120.3, 118.9, 118.7. Anal. calcd. for C₁₅H₁₀ClNO₂: C 63.04, H 4.07, Cl 14.31, N 5.67. Found C 63.10, H 4.13, Cl 14.28, N 5.58.

7c [X = CH₃]. *N*-(2,5-dihydroxybenzylidene)-*p*-methylaniline. The solvent was evaporated

with a nitrogen stream in a warm bath and the semisolid mixture was recrystallized twice from a mixture of benzene:cyclohexane (1:3). Yield: 81%; m.p.: 165 °C. ^1H NMR (Acetone- d_6): 12.54 (s, 1H, OH), 8.76 (s, 1H, HC=N), 7.93 (s, 1H, OH), 7.27 (m, 4H, aromatic H), 7.02 (d, $J = 2.8$ Hz, 1H, aromatic H), 6.93 (dd, $J = 8.8$ Hz and $J = 2.8$ Hz, 1H, aromatic H), 6.80 (d, $J = 8.8$ Hz, 1H, aromatic H), 2.35 (s, 3H, CH_3). ^{13}C NMR (Acetone- d_6): 163.7, 155.7, 150.9, 147.4, 137.9, 131.2, 122.3, 122.1, 120.6, 118.7, 118.6, 21.4. Anal. calcd. for $\text{C}_{14}\text{H}_{15}\text{NO}_2$: C 73.99, H 5.77, N 6.16. Found: C 73.80, H 5.80, N 5.95.

7d [X = CN]. N-(2,5-dihydroxybenzylidene)-*p*-cyanoaniline. A yellow precipitate was isolated by filtration from the reaction mixture, recrystallized in a mixture of benzene:acetonitrile:tetrachloroethane (1:2:2) and washed with pentane. Yield: 81 %; m.p.: 235 °C. ^1H NMR (Acetone- d_6): 11.98 (s, 1H, OH), 8.82 (s, 1H, HC=N), 8.03 (s, 1H, OH), 7.84 (d, $J = 8.3$ Hz, 2H, aromatic H), 7.54 (d, $J = 8.3$ Hz, 2H, aromatic H), 7.06 (d, $J = 2.8$ Hz, 1H, aromatic H), 7.00 (dd, $J = 8.8$ Hz and $J = 2.8$ Hz, 1H, aromatic H), 6.83 (d, $J = 8.8$ Hz, 1H, aromatic H). ^{13}C NMR (DMSO- d_6): 164.9, 153.2, 153.0, 149.8, 133.6, 122.5, 122.1, 119.4, 118.9, 117.4, 116.5, 108.6. Anal. calcd. for $\text{C}_{14}\text{H}_{10}\text{N}_2\text{O}_2$: C 70.58, H 4.23, N 11.76. Found: C 70.35, H 4.48, N 11.72.

7e [X = NO_2]. N-(2,5-dihydroxybenzylidene)-*p*-nitroaniline. A light brown solid was isolated from the reaction mixture by filtration and recrystallized from a mixture of benzene:acetonitrile:ethanol (1:5:1). Yield: 56 %; m.p.: 227 °C. ^1H NMR (Acetone- d_6): 11.95 (s, 1H, OH), 8.85 (s, 1H, HC=N), 8.34 (d, $J = 9.0$ Hz, 2H, aromatic H), 8.08 (s, 1H, OH), 7.62 (d, $J = 9.0$ Hz, 2H, aromatic H), 7.10 (d, $J = 2.9$ Hz, 1H, aromatic H), 7.03 (dd, $J = 8.8$ Hz and $J = 2.9$ Hz, 1H, aromatic H), 6.86 (d, $J = 8.8$ Hz, 1H, aromatic H). ^{13}C NMR (DMSO- d_6): 165.0, 155.0, 153.2, 149.8, 145.3, 125.0, 122.4, 119.5, 117.5, 116.3. Anal. calcd. for $\text{C}_{13}\text{H}_{10}\text{N}_2\text{O}_4$: C 60.47, H 3.90, N 10.85. Found: C 60.33, H 4.14, N 10.79.

7f [X = OEt]. N-(2,5-dihydroxybenzylidene)-*p*-ethoxyaniline. Yield: 65 %; m.p.: 140 °C (Lit. [5], m.p.: 142 °C). ^{13}C NMR (Acetone- d_6): 162.0, 159.5, 155.4, 150.8, 142.4, 123.4, 121.6, 120.5, 118.4, 118.3, 116.2, 64.5, 15.3.

7g [X = CF_3]. N-(2,5-dihydroxybenzylidene)-*p*-trifluoromethylaniline. The solvent was evaporated with a nitrogen stream in a warm bath and the semisolid mixture was recrystallized twice from a mixture of benzene:cyclohexane (1:6) to afford orange flakes. Yield: 85 %; m.p. 128 °C. ^1H NMR (Acetone- d_6): 12.10 (s, 1H, OH), 8.85 (s, 1H, HC=N), 8.05 (s, 1H, OH), 7.80 (d, $J = 8.5$ Hz, 2H, aromatic H), 7.58 (d, $J = 8.5$ Hz, 2H, aromatic H), 7.08 (d, $J = 2.9$ Hz, 1H, aromatic H), 7.01 (dd, $J = 8.7$ Hz and $J = 2.9$ Hz, 1H, aromatic H), 6.85 (d, $J = 8.7$ Hz, 1H, aromatic H). ^{13}C NMR (DMSO- d_6): 165.1, 153.4, 152.7, 150.0, 127.3, 127.2, 126.8, 126.7, 122.3, 122.1, 119.6, 117.6, 116.9. Anal. calcd. for $\text{C}_{14}\text{H}_{10}\text{F}_3\text{NO}_2$: C 59.79, H 3.58, N 4.98. Found: C 59.50, H 3.77, N 4.85.

Model compound synthesis. The model compounds **2a-g** were prepared by reaction of the hydroquinones **7a-g** (2.08 mmol) with para-*n*-hexyloxybenzoyl chloride (1.0 g, 4.15 mmol) in Cl_2CH_2 (50 ml) in the presence of Et_3N (1.2 ml) at room temperature and purified by several recrystallizations from ethanol. Yields of purified model compounds = 40-70%. **2a**. Anal. calcd. for $\text{C}_{39}\text{H}_{43}\text{NO}_6$: C, 75.33; H, 6.97; N, 2.25. Found: C, 75.02; H, 7.02; N, 2.11. **2b**. Anal. calcd. for $\text{C}_{39}\text{H}_{42}\text{ClNO}_6$: C, 71.38; H, 6.45; N, 2.14; Cl, 5.40. Found: C, 71.43; H, 6.54; N, 2.02; Cl, 5.35. **2c**. Anal. calcd. for $\text{C}_{40}\text{H}_{45}\text{NO}_6$: C, 75.56; H, 7.08; N, 2.20. Found: C, 75.43; H, 7.27; N, 2.28. **2d**. Anal. calcd. for $\text{C}_{40}\text{H}_{42}\text{N}_2\text{O}_6$: C, 74.28; H, 6.55; N, 4.33. Found: C, 74.34; H, 6.71; N, 4.43. **2e**. Anal. calcd. for $\text{C}_{39}\text{H}_{42}\text{N}_2\text{O}_8$: C, 70.25; H, 6.35; N, 4.20. Found: C, 70.18; H, 6.46; N, 4.05. **2f**. Anal. calcd. for $\text{C}_{41}\text{H}_{47}\text{NO}_7$: C, 73.96; H, 7.12; N, 2.10. Found: C, 74.19; H, 7.23; N, 2.17. **2g**. Anal. calcd. for $\text{C}_{40}\text{H}_{42}\text{F}_3\text{NO}_6$: C, 69.65; H, 6.14; N, 2.03; F, 8.26. Found: C, 69.78; H, 6.30; N, 2.00; F, 8.43.

Polymer synthesis and characterization. The polymers **1a-g** were prepared by reaction of **6**

with **7a-g** in CH_2Cl_2 solution in the presence of Et_3N as previously described [8]. The reaction was carried out at room temperature for 24 h, under reflux for additional 24 h and then cooled and poured into a five-fold excess of ethanol. The precipitated polymer was redissolved in methylene chloride and reprecipitated in ethanol. Then it was filtered, washed by a Soxhlet extraction with methanol and dried at 50 °C under vacuum. Yield: 92-95%. Since the GPC analysis indicated that variable amount of oligomers were present in the polymer samples, the higher molecular weight fraction of the polymers was isolated by fractional precipitation from THF-MeOH mixtures. **1a**, anal. calcd. for $\text{C}_{37}\text{H}_{37}\text{NO}_6$: C, 75.10; H, 6.30; N, 2.37. Found: C, 75.19; H, 6.55; N, 2.10. **1b**, anal. calcd. for $\text{C}_{37}\text{H}_{36}\text{ClNO}_6$: C, 70.97; H, 5.80; N, 2.24; Cl, 5.66. Found: C, 70.31; H, 6.20; N, 2.05; Cl, 5.70. **1c**, anal. calcd. for $\text{C}_{38}\text{H}_{39}\text{NO}_6$: C, 75.35; H, 6.49; N, 2.31. Found: C, 75.52; H, 6.65; N, 2.19. **1d**, anal. calcd. for $\text{C}_{38}\text{H}_{36}\text{N}_2\text{O}_6$: C, 74.01; H, 5.88; N, 4.54. Found: C, 74.11; H, 5.95; N, 4.35. **1e**, anal. calcd. for $\text{C}_{37}\text{H}_{36}\text{N}_2\text{O}_8$: C, 69.80; H, 5.70; N, 4.40. Found: C, 69.99; H, 5.91; N, 4.28. **1f**, anal. calcd. for $\text{C}_{39}\text{H}_{41}\text{NO}_7$: C, 73.68; H, 6.50; N, 2.20. Found: C, 73.14; H, 6.81; N, 2.09. **1g**, anal. calcd. for $\text{C}_{38}\text{H}_{36}\text{F}_3\text{NO}_6$: C, 69.18; H, 5.50; N, 2.12. Found: C, 69.27; H, 5.61; N, 2.07.

Molecular weights were determined using a Waters 201 GPC instrument calibrated with polystyrene standards and a 10 Å pore "µ-Styragel" column. Thermal analysis was carried out on a Du Pont 1090 DSC instrument under a nitrogen flow with a heating rate of 20 °C/min with polymer samples of about 10 mg. The peak maxima of the endothermic phase transitions were recorded from the second heating scan. The melt behavior was observed with a optical microscope equipped with cross-polarizers and a hot stage. All polymers showed the expected IR and NMR peaks.

Molecular Modeling. Molecular modeling of the compounds **2a-g** was carried out at the semiempirical level using AM1 MO program [14]. Modeling was assumed to be carried out in the gas phase at 0 °K. The minimization operations were performed using the conjugate gradient method and halted by setting the gradient option at 0.01 kcal/mol. The lowest potential energy conformations were found by minimization of the energy function in conjunction with conformation searches around various bonds.

Results and discussion

All the polymers synthesized were soluble in dichloromethane and the reaction mixtures remained homogeneous throughout the polymerization. However, high molecular weight samples ($M_w = 9000-14000$ Da, $M_w/M_n = 1.2-1.4$) were obtained only after fractional reprecipitation. Longer reactions times as well as larger scales and different polymerization solvents failed to increase the polymer molecular weight. The relatively low molecular weights of the as-prepared polymers, M_w : 3.800-8.000 Da, may be caused by the low reactivity of monomers **7a-g** which is probably due to intramolecular hydrogen bonding between the *ortho*-hydroxy group and the nitrogen of the azomethine structure [15].

The polarizing optical microscope (POM) observations and DSC measurements of the polyesters thermal properties are summarized in Table 1. Most of the polymers showed DSC curves with distinguishable melting and isotropization endothermic transition peaks. However, the DSC traces of polymers **1a** [X = H] and **1d** [X = CN] showed only one broad endothermic peak, although the typical nematic textures are observed both heating and cooling by polarized optical microscopy. From the optical microscope observations, polymer **1a** starts to melt at 116 °C, forms a nematic phase with a typical Schlieren texture with disclinations of both strength $|S| = 1$ and $|S| = 1/2$ at 135 °C and shows a maximum in the

DSC trace at 140 °C. This nematic melt becomes isotropic at 158 °C. Upon cooling, the isotropic melt forms a nematic state again at 152 °C. Therefore, the temperature range of this nematic phase in the heating cycle is narrow and the two endothermic melting and isotropization transitions overlap to give only one broad peak. Similar behavior was observed for polymer **1d** which starts to melt at 105 °C, shows a threaded texture at 115 °C, a maximum in the DSC trace at 128 °C and became isotropic at 144 °C.

Table 1. Molecular Weight and Thermal Properties of Polymers **1a-g**.

| [X] | GPC ^{a)} | | DSC (max.) ^{b)} /POM ^{c)} (°C) | | |
|----------------------|-------------------|--------------------------------|--|--------------------|------------------------------|
| | M _n | M _w /M _n | T _m | T _i | T _i ^{c)} |
| 1a = H | 13.000 | 1.3 | ^{d)} /145 | ^{d)} /158 | 152 |
| 1b = Cl | 8.500 | 1.4 | 123/123 | 136/148 | 141 |
| 1c = CH ₃ | 8.500 | 1.3 | 105/107 | 165/140 | 126 |
| 1d = CN | 8.800 | 1.4 | ^{d)} /100 | ^{d)} /128 | 120 |
| 1e = NO ₂ | 8.200 | 1.3 | 145/140 | 156/142 | 122 |
| 1f = OEt | 10.000 | 1.4 | 141/142 | 152/153 | 132 |
| 1g = CF ₃ | 7.400 | 1.2 | 84/84 | 105/110 | 100 |

a) After fractional reprecipitation in THF-MeOH. b) Thermal transition maxima observed in the second heating cycle. c) Thermal transition observed by POM in the second cooling cycle. d) Single very broad thermal transition.

All the other polymers **1** were enantiotropic as well and showed between the T_m and T_i either Schlieren or threaded textures typical of nematic mesophases. However, in addition to the common singularities with |S| = 1/2 or 1 that are often observed in polymeric nematic states, **1b** [X = Cl] showed singularities with 6 or 8 dark brushes corresponding to high strength disclinations of absolute S values 3/2 and 2. Though unusual, these high strength disclinations have been occasionally reported for single component nematic materials of both molecular [16] and macromolecular [17] nature.

The polymer **1** mesophase ranges shown in Table 1 are rather narrow as could be expected from the decrease of the axial ratio of the mesogenic group caused by the azomethine group attachment. Due to the narrowness of the mesophase ranges and the broad signals observed for the thermal transitions, the optical microscope observations should be considered to be more reliable than the DSC data in assessing the substituent effects on the mesophase thermodynamic stability.

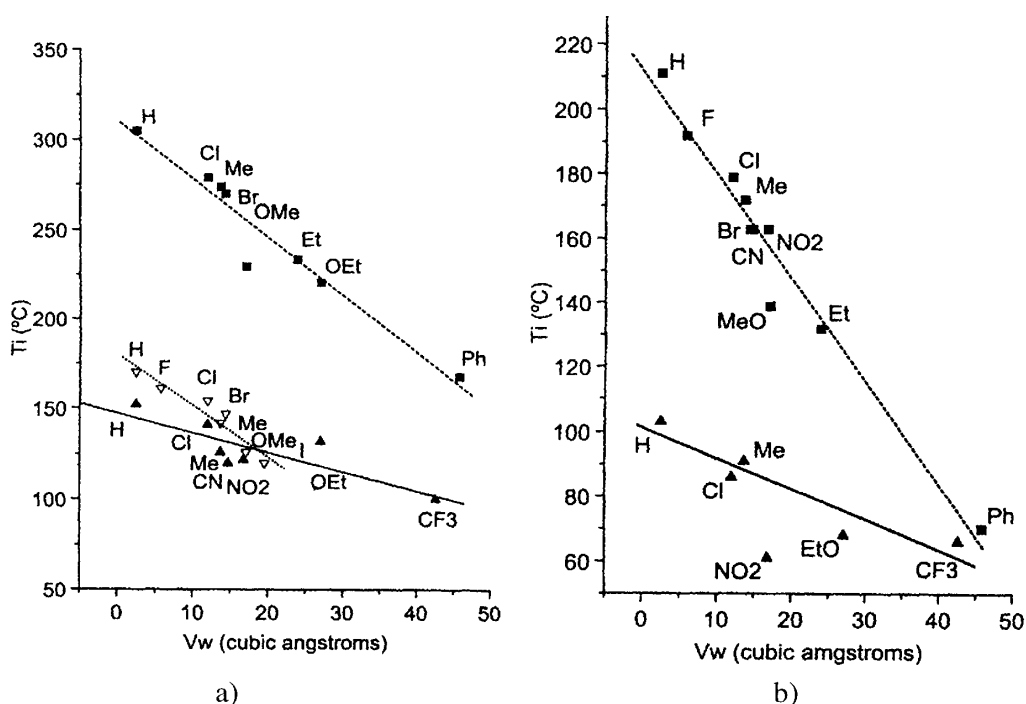


Figure 1. a) POM isotropization temperature, T_i , as a function of V_w for different substituents, X, on polymers series **1** (\blacktriangle), **3** (\blacksquare); X = H, Me, Cl, Br [7], X = OMe, OEt [8], X = Et [9], X = Ph [10] and **4** (\blacktriangledown) [11]. b) POM isotropization temperatures as a function of V_w for different substituents, X, on model compounds series **2** (\blacktriangle) and **5** (\blacksquare) [12].

Figure 1a presents T_i data of polymers **1** together with T_i data taken from previous studies on two related segmented liquid crystal polymers series series **3** [7,8,9,10] and series **4** [12]. T_i values were plotted against substituent van der Waals volumes, V_w , instead of van der Waals radii, r_w , because the former account better for intermolecular distance variations due to substituent changes which in turn are related to steric, dispersive and polar intermolecular interactions [18]. Figure 1a shows that the isotropization temperature of the nematic phases of polymers **1** decrease systematically as the size the substituents increase. Besides, it is possible to estimate the susceptibility of the mesophase stability to substituent steric effects from the slope of the linear correlations. The mesophase stability of the polymer series **1** (slope, $s = -1.07$, correlation coefficient, $r = -0.826$) is less affected by the substituent nature than those corresponding to polymer series **3** ($s = -3.23$, $r = -0.997$) and polymer series **4** ($s = -2.83$, $r = -0.985$). Clearly, and despite the different mesogenic core structures of polymers **3** and **4**, the full steric effect is operating in these two polymer series since the substituent groups protrude from the aryl rings out of the polymer main chain. On the contrary, the conformational flexibility of the pendant azomethine group in polymers **1** could allow the *p*-aryl substituents to be partially aligned along the longitudinal axis of the mesogenic unit, thus diminishing the effects due to the lateral substituent size. As a matter of fact, this explanation was supported by computer modeling studies done on model compounds **2** which mimic polymers **1** repeating units. Thus, after a conformational search at the semiempirical quantum mechanical level using the AM1 MO program, it was found that the two more stable conformations are the ones shown in Figure 2a and 2b. Moreover, the calculated heats of

formation which are shown in Table 2 for both the folded, H_f^F , and the extended, H_f^E , conformers indicate that the folded conformations are predominant and that their contribution to the conformational equilibria between folded and extended conformations is significant.

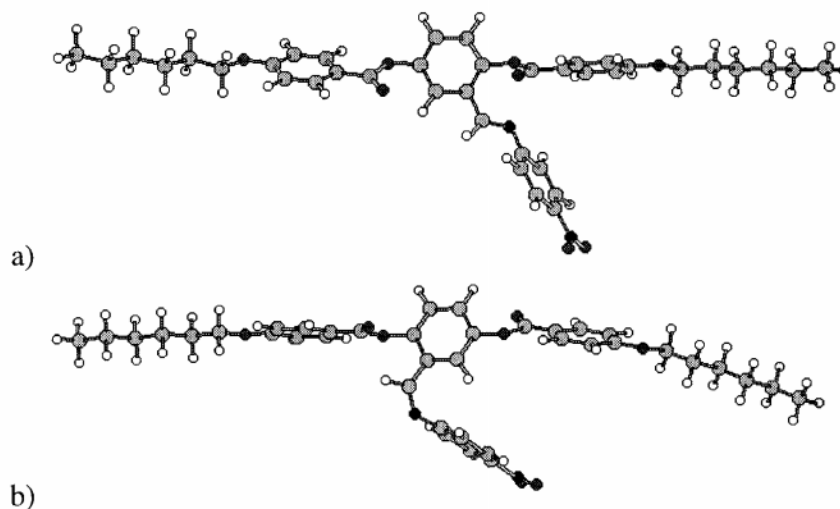


Figure 2. AM1 geometries of the a) extended and b) folded conformations of **2e**.

Table 2. Van der Waals volumes of X, V_w , and calculated heat of formation of the folded, H_f^F , and the extended, H_f^E , conformations of model compounds 2a-g

| Model Compound | V_w (\AA^3) ^{a)} | H_f (Kcal/mol) ^{a)} | | ΔH_f (Kcal/mol) |
|-------------------------|--|--------------------------------|---------|-------------------------|
| | | H_f^F | H_f^E | $H_f^F - H_f^E$ |
| 2a, X = H | 2.5 | -151.9 | -150.6 | - 1.3 |
| 2b, X = Cl | 12.0 | -159.1 | -157.8 | - 1.3 |
| 2c, X = CH ₃ | 13.7 | -159.5 | -158.3 | - 1.2 |
| 2d, X = CN | 14.7 | -120.9 | -119.4 | - 1.5 |
| 2e, X = NO ₂ | 16.8 | -149.6 | -147.8 | - 1.8 |
| 2f, X = OEt | 27.1 | -195.0 | -194.1 | - 0.9 |
| 2g, X = CF ₃ | 42.6 | -308.5 | -307.1 | - 1.4 |

a) All V_w values were taken or calculated from data of ref. 19 with the exception of V_w for X = CF₃ which was taken from ref. 20.

In addition, the model compounds **2a-g** were synthesized and their thermal properties were analyzed by DSC and POM in order to compare their thermotropic properties to those of polymers **1**. Only **2d** [X = CN] showed no mesomorphic properties. All others model compounds **2** are nematic monotropic. Figure 1b presents T_i data of model compounds **2** together with T_i data of the related model compound series **5** which was taken from previous reports [12]. Both series **2** ($s = -0.89$, $r = -0.744$) and **5** ($s = -3.22$, $r = -0.981$) showed relationships between mesophase stability and V_w data similar to that observed for most of

the nematic low-molecular-weight compounds even though the linear correlation for **2** is more scattered. The clearing temperatures behavior in nematic compounds depend on steric and occasionally on dispersive effects, with dipolar effects playing no role the polymer mesomorphic behavior. As observed before for the polymer series, the mesophase stability of the model compound series **2** with the arylazomethine group is less affected by the substituent nature than those corresponding to series **5** where the substituent is directly attached to the central mesogenic core.

Noteworthy, the segmented polymer **1** and its model compounds **2** showed similar susceptibilities of their mesophase thermodynamic stability to steric effects as well as the segmented polymer **3** and its model compounds **5** did. Therefore, it can also be concluded that the mesomorphic behavior of model compounds can be used to estimate polymer mesomorphic properties when steric effects are predominant. Besides, this study suggests that due to the conformational flexibility of the azomethine group this type of polymers cannot be strictly considered as Y-shaped segmented liquid crystal polymers.

Acknowledgements

We are deeply indebted to R. W. Lenz for financial support and advice. Additional financial support provided by CONICET, ANPCyT and SGCyT-UNS (Argentina) and by the NNSF and the "863" project of China is also appreciated.

References

1. Demus D (1989) *Liquid Cryst* 5:75
2. Tschierske C (1998) *J Mater Chem* 8:1485
3. Berg S, Krone V, Ringsdorf H (1986) *Makromol Chem, Rapid Commun* 7:381
4. Zhou Q-F, Wu X, Wen Z (1989) *Macromolecules* 22:491
5. Zhou Q-F, Wu Z-C, Lenz RW (1991) *Polym Bull* 27:257
6. Fischer H, Rötz U, Lindau J, Mädicke A, Kuschel F (1992) *Polym Bull* 27:657
7. Lenz RW (1985) *Polymer J.* 17:105
8. Bhowmik PK, Garay RO, Lenz RW (1991) *Makromol Chem* 192:415
9. Antoun S, Lenz RW, Jin J-I (1981) *J Polym Sci, Polym Chem Ed* 19:1901
10. Jo BW, Lenz RW, Jin J-I (1982) *Makromol Chem, Rapid Commun* 3:23
11. Furukawa A, Lenz RW (1986) *Macromol Chem, Macromol Symp* 2:3
12. Demus D, Zashcke H, editors (1984) *Flussige Kristalle in Tabellen II*, Leipzig: VEB Deutscher Verlag für Grundstoffindustrie.
13. Griffin AC, Havens SJ (1981) *J Polym Sci, Polym Phys Ed* 19:951
14. Hypercube Inc (1997) *Hyperchem for Windows*, Release 5.1
15. Teucher I, Paleos CM, Labes MM (1970) *Mol Cryst Liq Cryst* 11:187
16. Viney C, Brown DJ, Dannels CM, Twieg RJ (1993) *Liq Cryst* 13:95
17. Song W, Chen S, Qian R (1993) *Makromol Chem, Rapid Commun* 14:605
18. Osman MA (1985) *Mol Cryst Liq Cryst* 128:45
19. Bondi A (1964) *J Phys Chem* 68:441
20. Seebach D (1990) *Angew Chem Int Ed Engl* 29:1320